

## Effects of hydrostatic pressure on the fundamental absorption edge of TlGaSe<sub>2</sub>

S. Ves

Department of Physics, Solid State Section, Aristotle University of Thessaloniki, GR-54 006, Thessaloniki, Greece  
(Received 8 March 1989)

The effect of hydrostatic pressure on the lowest direct gaps  $E_a$  ( $\Gamma_2^v \rightarrow \Gamma_{3,2}^c$ ) and  $E_b$  ( $\Gamma_2^v \rightarrow \Gamma_{3,1}^c, \Gamma_1^c$ ) of TlGaSe<sub>2</sub> has been investigated by optical-absorption measurements in a diamond-anvil cell for thin (3.5–20  $\mu\text{m}$ ) samples at room temperature and for pressures up to 12.0 GPa. Sublinear and linear red shifts have been observed for the  $E_a$  and  $E_b$  gaps, respectively. The results are indicative of a possible phase transition at about 1.85 GPa. The present results are discussed in light of related experimental and theoretical studies.

### I. INTRODUCTION

Recently, a lot of interest<sup>1–25</sup> has been drawn to the ternary semiconducting chalcogenides of the  $A^{III}B^{III}C_1^{VI}$  type ( $A, B$  represent metal atoms and  $C$  chalcogen atoms). They are layer and chain crystals and exhibit strong anisotropy, clearly manifested in their mechanical properties. TlGaSe<sub>2</sub> belongs to this class and it is one of the most intensively studied members of this family.<sup>1–25</sup> The crystal structure (Fig. 1) of this compound has been investigated thoroughly in Ref. 10 (and references therein) and has been shown that single crystals of TlGaSe<sub>2</sub> have the monoclinic structure and the  $C_{2/c}$  ( $C_{2h}^6$ ) space group.

TlGaSe<sub>2</sub> exhibits strong excitonic effects<sup>1,3,5,8,9,15,19,21</sup> observed even at room temperature.<sup>1,3,5</sup> Their polarization dependence<sup>9,19,20</sup> has not been clearly understood up to now and the available experimental data are not free of contradictions.<sup>9,19,20</sup> Besides that, the TlGaSe<sub>2</sub> compound is also of great interest because of the relatively large number, four, of phase transitions induced by temperature in the range 4.2–294 K.<sup>10,13,15,16,19–21,25</sup> Despite the use of different techniques to study the temperature-induced phase transitions in TlGaSe<sub>2</sub> crystals, it is still impossible to establish the mechanisms of the structural transformations and the structural features in the low-temperature phases.

In contrast to the temperature-induced phase transitions, the information about the pressure effect on this crystal is limited<sup>4,6,10,14,18</sup> and mostly restricted to pressures up to 1 GPa. In addition, there is no agreement among the published experimental data. Thus, Vinogradov *et al.*,<sup>6</sup> using Raman spectroscopy, reported a phase transition at room temperature and at about 0.5 GPa, while Henkel *et al.*,<sup>10</sup> also from Raman data, found no indication of any phase transition in this pressure region. Furthermore, Allakhverdiev *et al.*<sup>14</sup> present a qualitative temperature-pressure phase diagram of TlGaSe<sub>2</sub>, in which a phase transition at 0.5 GPa and room temperature is shown, but transmission measurements under pressure,<sup>18</sup> up to 1.27 GPa, did not reveal any peculiarity of the absorption-edge shift in this pressure region. Recently, theoretical calculations using the pseudopotential

method of the band structure of TlGaSe<sub>2</sub> have been reported.

In this paper we present detailed absorption measurements of the full absorption-edge profile in the vicinity of the related critical points on well-characterized samples of TlGaSe<sub>2</sub> as a function of hydrostatic pressure up to 12 GPa. Thus, the influence of pure hydrostatic pressure on the absorption-edge profile and indirectly on the band structure is investigated as well as the occurrence of pressure-induced phase transitions in this pressure range. This method has been proved to be one of the most sensitive techniques, at least in the case of the classical IV, III-V, II-VI, and I-VII semiconductor families.<sup>26–33</sup> Our results are compared with previous theoretical and experimental data.

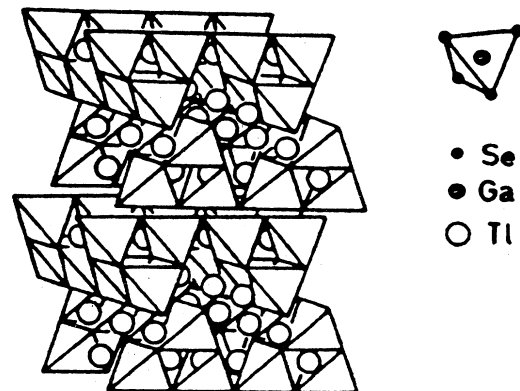


FIG. 1. Stacking of anionic layers and positions of Tl<sup>+</sup> ions between them. The  $B_4X_{10}$  polyhedra ( $B$  represents metal atoms,  $X$  represents chalcogen atoms) are built up adamantine-like by four  $BX_4$  tetrahedra with common corners. These  $B_4X_{10}$  polyhedra are condensed with four neighboring polyhedra by common corners forming a  $\frac{2}{3}(BX_2)$  layer parallel to (001). The upper and lower edges of these adamantine-like units point in the [110] and  $[\bar{1}10]$  directions. Two such layers are stacked in the cell along [001]. Succeeding layers are twisted 90° to each other, forming trigonal prismatic voids.

## II. EXPERIMENT

Optical-absorption measurements under pure hydrostatic pressures up to 13 GPa were performed in a gasketed diamond-anvil cell<sup>34</sup> at room temperature. The crystal preparation has been described elsewhere.<sup>10</sup> The samples were mechanically polished down to thicknesses of 3.5 or 20  $\mu\text{m}$ . A sufficiently small sample piece, measuring about 100  $\mu\text{m}$  across, was inserted, together with several ruby chips into the hole of a 95- $\mu\text{m}$ -thick hard steel (Rhemanit) gasket resting flat on the lower diamond. The hole diameter was about 200  $\mu\text{m}$ . A 4:1 mixture of methanol and ethanol was used as a pressure-transmitting medium. The pressure was measured using the standard ruby fluorescence technique.<sup>34,35</sup> The data were taken over a period of several days and the pressures given are the mean values of initial and final ones for each run, which differ typically by less than 0.1 GPa. The maximum pressure gradient across the gasket hole was less 0.05 GPa as checked by measuring the pressure from several ruby chips distributed across the gasket hole. The measurements were carried out, in both cases, in the E||C geometry. Here E and C denote the vector of the electric field of the incident light and the axis perpendicular to the layer plane, respectively.

The absorption coefficient was obtained by normalizing the transmission through the sample to the transmission through a clear area next to the sample. No corrections for reflection losses at the interfaces between the sample and the pressure medium were taken into account. This gave us a remaining, nearly constant, small absorption background. The beamspot size was smaller than that of the sample (100  $\mu\text{m}$ ) diameter. This was achieved by illuminating a 100- $\mu\text{m}$ -diam pinhole with a Xe 75-W high-pressure lamp imaging it onto the sample by an achromatic uv-lens. With careful alignment, to ensure on-axis operation, a 20- $\mu\text{m}$  image of the pinhole was obtained on the sample. In this way the scattered light due to multiple reflections was considerably suppressed. In order to reduce even more the "spurious light," the light leaving the cell was again focused through a 20 $\times$  demagnification uv-achromat on a second pinhole with a diameter of 100  $\mu\text{m}$ . Thus we could select a region of the illustrated area of the sample. Finally, the radiation leaving the second pinhole was collected by an uv-achromat and focused onto the entrance slit of a  $\frac{3}{4}$ -m Jobin Yvon 640 monochromator. The spectral resolution was about 1  $\text{\AA}$ . A C31034 RCA photomultiplier tube and a fast photon-counting system connected to a personal computer was used to measure the intensity of the transmitted light.

## III. RESULTS AND DISCUSSION

In Figs. 2 and 3 we have plotted typical absorption spectra of TlGaSe<sub>2</sub> as a function of spectral energy at room temperature for a crystal of thickness 3.5  $\mu\text{m}$  in the low-, up to 2.87 GPa, and in the high-, up to 11.4 GPa, pressure regimes, respectively. From Fig. 2 it is clear that for low pressures, the absorption edge shows a two-step shape, implying the contribution of at least two tran-

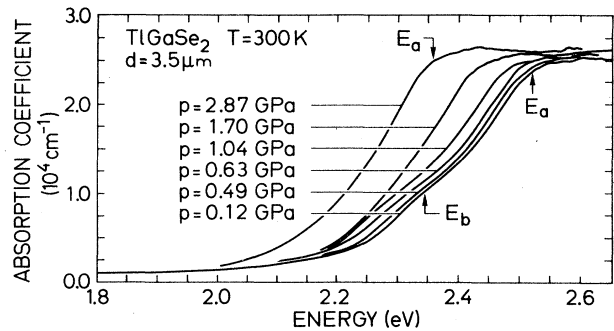


FIG. 2. Typical absorption spectra of the lowest transitions of TlGaSe<sub>2</sub> at room temperature for various pressures in the low-pressure regime. The arrows indicate the saturation points taken to be the "exciton edges" at the given pressure. The thickness of the sample is 3.5  $\mu\text{m}$ .

sitions. (We will comment on this point later on.) At pressures about 1.85 GPa, the absorption edges change form and do not show the first kink anymore. In the remaining pressure ranges investigated, the absorption coefficient curves show a clear uniform red shift without any other change in their shape, as can be seen from Fig. 3. Furthermore, we should stress the fact that the change of the shape of the absorption coefficient curve upon pressure is completely reversible upon increasing or decreasing pressure. The arrows indicate the saturation point taken to represent the gap energy. These energies were determined from the minimum of the second derivative of the absorption spectra with respect to photon energy.

In Fig. 4 we display typical absorption coefficient curves of a thicker sample ( $d=20 \mu\text{m}$ ). The corresponding gap energy has been determined again by the second-derivative method. For this sample, the absorption coefficient rises smoothly and gradually as a function of the photon energy and the first kink is hardly seen. Also, the maximum absorption coefficient curve saturates at values lower than those corresponding to absorption resulting from direct transitions, as will be discussed later. This premature saturation effect observed in Figs. 2–4 is

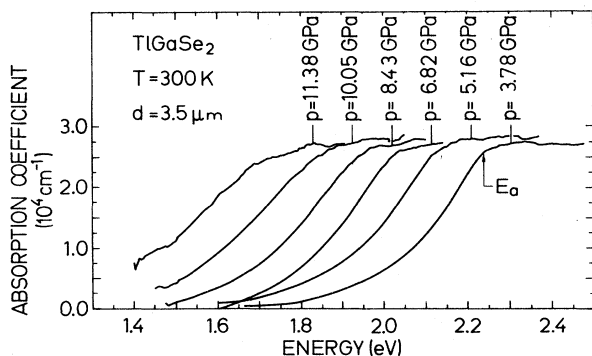


FIG. 3. The same as Fig. 3 but for the high-pressure regime.

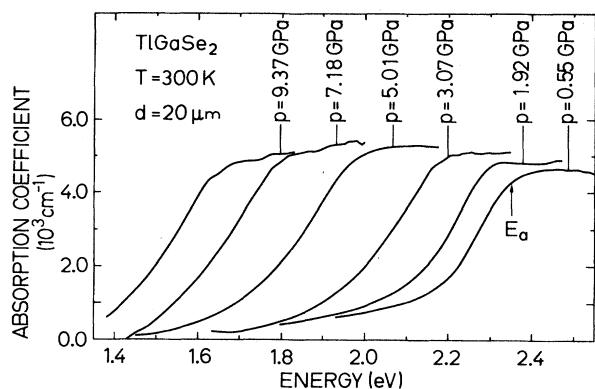


FIG. 4. Absorption spectra of a 20- $\mu\text{m}$ -thick sample of  $\text{TiGaSe}_2$  obtained at room temperature for several hydrostatic pressures up to 9.4 GPa, in the region of the lowest direct gap.

a common feature to most measurements performed in the diamond-anvil cell with samples prepared from bulk crystal and is due to the unavoidable spurious scattered light.<sup>26–29</sup> We take, nevertheless, these points (arrows in Figs. 2–4) as a measure of the absorption-edge energy versus pressure. From Figs. 2 and 4 it is clear that the thinner the sample used, the closer the appearance of the saturation point in the absorption-coefficient curve to the corresponding transition energy. Thus the error due to the effect just mentioned is assumed to be a small constant offset to lower energies.

The corresponding energy values of the gaps as  $E_a$  and  $E_b$ , and obtained in the way mentioned above from Figs. 2–4, are plotted as a function of pressure in Fig. 5. The crosses and the open circles represent measurements obtained from a thin sample ( $d = 3.5 \mu\text{m}$ ), while the solid

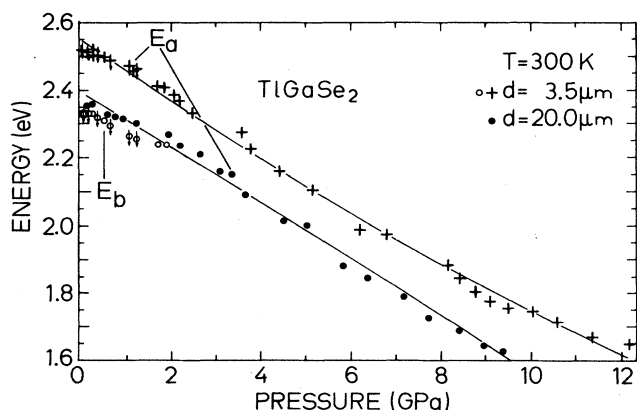


FIG. 5. The shift in the absorption edge of  $\text{TiGaSe}_2$  vs hydrostatic pressure at room temperature. Points marked with crosses and open circles are from Figs. 2 and 3, while the solid circles are from Fig. 4. Points marked with  $\downarrow$  indicate decreasing pressure. The solid lines through the experimental data represent quadratic or linear least-squares fits, for the  $E_a$  and  $E_b$ , respectively.

circles from a thicker one ( $d = 20 \mu\text{m}$ ). Experimental data marked with an arrow ( $\downarrow$ ) correspond to runs with decreasing pressure. The solid lines through the experimental data represent a quadratic fit to them. Although the energy position of the saturation point for the 20- $\mu\text{m}$ -thick samples is much closer to the  $E_b$  gap, we associate it to the  $E_a$  energy gap by considering the fact that the maximum values reached for the absorption coefficient are, roughly speaking, half an order of magnitude smaller than that corresponding to direct transitions ( $3 \times 10^4 \text{ cm}^{-1}$ ). This kind of association is also supported by the pressure dependence of the two edges, which is similar throughout the whole pressure region. The linear and quadratic pressure coefficients of the  $E_a$  and  $E_b$  gaps are listed in Table I. They were obtained from a least-squares fit to the experimental data with a polynomial. As can be seen from Table I, there exist some scattering in the values of the  $E_a$  and  $E_b$  gaps, reflecting the discrepancies arising from differences in the interpretation of the observed absorption-edge profile. The same difficulties occur also in well-studied semiconductors, such as Ge (Ref. 26) and GaAs (Ref. 27), where, due to the use of thick samples, it was not possible to measure the whole absorption-edge profile. In a similar fashion, difficulties arise also in cases where more than one transition is involved [GaP (Ref. 28) and AlSb (Ref. 29)]. The common feature of such kind of measurements is that they lead to a thickness dependence of the energy gap. Therefore, we believe that our values of  $E_a = 2.547 \pm 0.007 \text{ eV}$  and  $E_b = 2.344 \pm 0.001 \text{ eV}$  obtained from samples with a thickness of  $3.5 \mu\text{m}$  are more accurate. These discrepancies, however, do not arise for the pressure coefficients, where the experimental values are in agreement, within experimental error. The apparent discrepancy of the linear pressure coefficient determined from the thin and thick samples arises mainly from the different kind of curve used in the fitting. Thus, for a pure linear fitting in the thin-sample data, the coefficient

TABLE I. Coefficients of the least-squares fits with  $E(p) = E_0 + bp + cp^2$  to the experimental pressure dependence of the  $E_a$  and  $E_b$  gaps of  $\text{TiGaSe}_2$  at room temperature.

|       | $E_0$ (eV)                | $b$ ( $10^{-2} \text{ eV/GPa}$ ) | $c$ ( $10^{-4} \text{ eV/GPa}^2$ ) |
|-------|---------------------------|----------------------------------|------------------------------------|
| $E_a$ | $2.547 \pm 0.007^a$       | $-92.2 \pm 4^a$                  | $1.23 \pm 0.04^a$                  |
|       | $2.397 \pm 0.01^b$        | $-83.3 \pm 5^b$                  |                                    |
|       | $2.384^c, 2.39^f$         |                                  |                                    |
| $E_b$ | $2.344 \pm 0.004^a$       | $-73.3 \pm 4^a$                  |                                    |
|       | $2.22 \pm 0.05^d$         | $-72.5 \pm 3^d$                  |                                    |
|       | $2.1^c, 2.23^e$           |                                  |                                    |
|       | $2.15^g, 2.18 \pm 0.02^h$ |                                  |                                    |

<sup>a</sup>This work, thickness  $d = 3.5 \mu\text{m}$ ,  $T = 300 \text{ K}$ .

<sup>b</sup>This work, thickness  $d = 20 \mu\text{m}$ ,  $T = 300 \text{ K}$ .

<sup>c</sup>Ref. 3, thickness  $d = 20\text{--}200 \mu\text{m}$ ,  $T = 300 \text{ K}$ .

<sup>d</sup>Ref. 18, thickness  $d = 30\text{--}60 \mu\text{m}$ ,  $T = 300 \text{ K}$ .

<sup>e</sup>Ref. 5, thickness  $d = 30\text{--}50 \mu\text{m}$ ,  $T = 300 \text{ K}$ .

<sup>f</sup>Ref. 19, thickness  $d = 20\text{--}150 \mu\text{m}$ ,  $T = 1.8 \text{ K}$ .

<sup>g</sup>Ref. 8, thickness  $d = 180 \mu\text{m}$ ,  $T = 100 \text{ K}$ .

<sup>h</sup>Ref. 1, thickness  $d = 150 \mu\text{m}$ ,  $T = 300 \text{ K}$ .

(in meV/GPa)  $b = -92.2 \pm 4$  becomes  $-79 \pm 4$ , comparing well with  $-83.3 \pm 5$ .

In the following we will try to assign the observed energy gaps to the corresponding transitions based on theoretical band-structure calculations. As already mentioned, the TlGaSe<sub>2</sub> crystallizes in the monoclinic structure  $C_{2h}^6$  with 16 formula units in two layers per unit cell. The band structure of this monoclinic TlGaSe<sub>2</sub> has been calculated<sup>11,23</sup> using the pseudopotential method with a convergence of 0.2 eV for the levels located near the forbidden gap.

According to the above calculations,<sup>23</sup> the top of the valence band is located at the  $\Gamma$  point with a symmetry  $\Gamma_2^c$ , while the absolute minimum of the conduction band is located in a distance of about  $\frac{1}{4}$  away from the  $\Gamma$  point along the  $\Gamma$ - $Y$  line ( $\Delta$  line). An additional extremum of the first conduction band is located at the  $\Gamma$  point with a symmetry  $\Gamma_{3,1}^c$ . The energy difference between these two extrema is approximately 120 meV. The next minimum at the  $\Gamma$  point is lying about 50 meV above the  $\Gamma_3^c$  and has the symmetry  $\Gamma_1^c$ . The third minimum of the conduction band, still at the  $\Gamma$  point, also possesses the symmetry  $\Gamma_{3,2}^c$  and it is located about 250 meV above the first  $\Gamma_{3,1}^c$  minimum. The lowest direct gap is about 2.1 eV and corresponds to the  $\Gamma_2^v \rightarrow \Gamma_{3,1}^c$  transition. Within the dipole approximation the  $\Gamma_2^v \rightarrow \Gamma_{3,1}^c$  and  $\Gamma_2^v \rightarrow \Gamma_1^c$  are allowed in the  $\mathbf{E} \parallel \sigma$  and  $\mathbf{E} \perp \sigma$  configurations, respectively ( $\mathbf{E}$  and  $\sigma$  designate the electrical vector of the incident light and the reflection plane, respectively). By including spin effects both transitions become allowed. Since in our experiments the light was unpolarized and incident perpendicular to the layer plane, all the above-mentioned transitions were allowed. Under these circumstances and taking into account the fact that the strength of the absorption coefficient, at least for the thin samples, is of the order of  $10^4 \text{ cm}^{-1}$ , we attribute the  $E_a = 2.547 \pm 0.007$  eV gap to transitions occurring between the  $\Gamma_2^v \rightarrow \Gamma_{3,2}^c$  band, while the  $E_b = 2.344 \pm 0.004$  eV gap must be resulting from both kinds of transitions,  $\Gamma_2^v \rightarrow \Gamma_{3,1}^c$  and  $\Gamma_2^v \rightarrow \Gamma_1^c$ , not resolved in our measurements at room temperature. All these transitions have been resolved at liquid-helium temperature,<sup>9,19,20</sup> although their polarization dependence is not well understood in terms of the  $C_{2h}^6$  symmetry.<sup>23</sup> In the case of the thicker samples we see only part of the steeply rising absorption edge and the first knee is hardly seen, due to the fact that at this photon energy the contribution of the indirect transitions  $\Gamma_2^v \rightarrow \Delta^c$  is no longer negligible for the following two reasons: First, the thickness of the crystal is now 6 times larger, and second, the photon energy of 2.2 eV is well above the threshold energy of the indirect transition  $\Gamma_2^v \rightarrow \Delta^c$  at 2.05 eV.<sup>3,5,8,9</sup> These phenomena taken together cause a very complex absorption-edge shape which, along with the also complicated band structure and, in particular, the lack of required data, make any attempt for an analysis similar to that of Ref. 29 unreasonable.

As already mentioned, the pressure dependence of the  $E_a$  and  $E_b$  gaps show, for the thin as well as the thicker samples, a negative pressure dependence which exhibits a sublinearity for the thin samples, at very high pressures.

To interpret these results for the band-gap pressure coefficient, we should first note that pressure coefficients are generally positive for three-dimensional-network covalent semiconductors with a direct band gap,<sup>26-33</sup> while a negative value of  $dE_g/dp$  has been found not only for TlGaSe<sub>2</sub> but also for other layer-structure semiconductors such as As<sub>2</sub>S<sub>3</sub>,<sup>36</sup> black P,<sup>37</sup> TlSe,<sup>38</sup> GaSe,<sup>39</sup> TlInSe<sub>2</sub>,<sup>40</sup> TlGaS<sub>2</sub>,<sup>18</sup> and Se;<sup>41</sup> that is, solids with a network dimensionality less than 3. Especially for the case of TlGaSe<sub>2</sub>, a qualitative explanation can be given based on the so-called closed-shell interactions<sup>41-43</sup> and considering the structure (Fig. 1) of the TlGaSe<sub>2</sub> crystals. Thus, a decrease in the Ga—Se bond length in the Ga<sub>4</sub>Se<sub>10</sub> polyhedra, built up adamanelike by four GaSe<sub>4</sub>, makes the bonding stronger and gives rise to an increase of the energy gap through an increase of the energy separation between the orbitals forming the lower conduction band  $E^c$  and the higher valence band  $E^v$ . On the other hand, a decrease of the interlayer distance makes the interlayer interaction, realized here by the Tl atoms between the layers, strong and gives rise to a decrease of the energy gap through an increase of the band dispersion in the layer-stacking direction ( $\Gamma$ - $Z$ ) (a fact well depicted in Fig. 2 of Ref. 23). Because of the weakness of the interlayer interactions compared with the intralayer interactions, the latter effect is expected to be much larger than the former one and the pressure coefficient of the energy gap has a large negative value, depending on the strength of the interlayer interactions. The fact that the obtained values of  $b = -92.2 \pm 4$  for the pressure coefficient of TlGaSe<sub>2</sub> is smaller by a factor of almost 2, compared to those obtained for typical layer materials in (meV/GPa) as As<sub>2</sub>S<sub>3</sub> =  $-140 \pm 3$ ,<sup>36</sup> black P =  $-167$ ,<sup>37</sup> PbI<sub>2</sub> =  $-165 \pm 6$ ,<sup>42</sup> Se =  $-225$ ,<sup>36</sup> TlSe =  $-150$ ,<sup>38</sup> and much closer to that of TlGaS<sub>2</sub> =  $-85.5 \pm 2.5$ ,<sup>18</sup> TlInS<sub>2</sub> =  $-85 \pm 2$ ,<sup>18</sup> is a strong indication, confirming the findings of Ref. 10, where a hierarchy of the bonding forces has been revealed, rather than only strong intralayer and weak interlayer bonds. The bending up of the  $E_b$  gap at high pressures suggests that at these pressures the interlayer interaction becomes comparable to the intralayer one, so that both of them play an essential role, forcing a tendency from two-dimensional to three-dimensional behavior observed also in As<sub>2</sub>S<sub>3</sub> (Ref. 36) and  $\alpha$ -As<sub>2</sub>S<sub>3</sub>.<sup>41</sup>

Within this context one might argue that the corresponding refractive index should increase with pressure as the electronic gap decreases. A similar behavior has been observed in  $\alpha$ -As<sub>2</sub>S<sub>3</sub>,<sup>41</sup> while the opposite behavior, i.e., a decreasing of the refractive index versus pressure, has been observed in semiconductors with a zinc-blende structure.<sup>33,44,45</sup> For the sake of completeness, we mention that a negative linear pressure coefficient has been observed also for the  $\Gamma^v \rightarrow X^c$  edge of other tetrahedrally coordinated semiconductors. The negative sign of the linear pressure coefficient of the  $\Gamma \rightarrow X$  transition results from a lowering of the  $X$  state and an increase of the  $\Gamma$  state upon decreasing volume, a situation predicted by calculation also in the layered TlSe for the direct  $T_4 \rightarrow T_3$  transitions.<sup>45</sup>

Next, we discuss the pressure dependence of the absorption edge. From Fig. 2 it is evident that our experimental results do not support the assumption of a structural phase transition around 0.5 GPa, reported in Refs. 6 and 14. A similar behavior around 0.5 GPa has also been reported by Allakhverdiev *et al.*<sup>18</sup> In this paper a change of the absorption-edge shape in the opposite direction has been found, i.e., two bends appear around 1.25 GPa, which are attributed to contributions of transitions into exciton or impurity states. On the contrary, our experimental data, mainly from the thin sample, indicate that if any phase transition would occur, it should take place around 1.85 GPa. This assumption is based on the fact that the  $E_b$  gap disappears for higher pressures. However, it is strange that the pressure dependence of the  $E_a$  gap does not show discontinuity or a considerable change in the slope in this pressure region. At this point we should mention that the same behavior as in Figs. 2–4 for  $E_a$  and  $E_b$  versus pressure is observed if we plot the absorption coefficient at constant values, e.g., at  $1.7 \times 10^4$  and  $7.5 \times 10^3 \text{ cm}^{-1}$ . Also, Raman measurements on TlGaSe<sub>2</sub> at room temperature and for pressures up to 2.1 GPa (Ref. 10) do not indicate any structural phase transition. Under these circumstances we believe that if any “transition” takes place it should be considered as a slight rearrangement of the crystal with a very small deformation necessary for a change of the symmetry from the  $C_{2h}^6$  to the new one. For such a small rearrangement, the transition corresponding to the  $E_a$  energy gap should be left almost unchanged. On the other hand, it is known that application of high pressure and high temperature ( $p_0 > 2 \text{ GPa}$ ,  $T_0 > 600^\circ\text{C}$ ) transforms the monoclinic TlGaSe<sub>2</sub> to the tetragonal TlSe-type structure ( $D_{4h}^{18}$ ).<sup>4</sup> The band structure of the tetragonal TlGaGe<sub>2</sub>, calculated using the pseudopotential method,<sup>11</sup> shows that in this structure the fundamental gap is also a direct one and it corresponds to the  $T_3^v \rightarrow T_4^c$  transition with an energy of 1.3 eV. This energy, however, is much less than that of 2.4 eV, which corresponds to 2 GPa. But, on the other hand, the  $T$  point of the  $D_{4h}^{18}$  symmetry transforms to the

$\Gamma$  point in the  $C_{2h}^6$  symmetry, which supports the idea of leaving the character of this transition unchanged. In view of these facts, this kind of transition could be a possibility, but taking into account that the temperature of our experiments,  $T = 300 \text{ K}$ , was much lower than that of  $T_c > 870 \text{ K}$  renders it less probable, but not impossible. Nevertheless, we believe that an unambiguous answer to this question would be provided only by x-ray measurements under pressure.

#### IV. CONCLUSION

In the present work using the diamond-anvil-cell technique we have measured the effect of pressure, at room temperature, on the optical-absorption edge of TlGaSe<sub>2</sub>. With increasing pressure the optical band gaps red shift rapidly, decreasing from 2.54 eV at  $p = 0$  to 1.65 eV at 12 GPa for the  $E_a$  gap and from 2.34 eV at  $p = 0$  to 2.19 eV at 2 GPa. The energy-gap shifts follow the expressions  $E_a(\text{eV}) = (2.547 \pm 0.007) - (92.2 \pm 4) \times 10^{-2} p + (1.23 \pm 0.04) \times 10^{-4} p^2$  and  $E_b(\text{eV}) = (2.344 \pm 0.004) - (73.3 \pm 4) \times 10^{-2} p$  ( $p$  in GPa). The optical band gaps  $E_a$  and  $E_b$  have been assigned to the corresponding interband  $\Gamma_2^v \rightarrow \Gamma_{3,2}^c$  and  $\Gamma_2^v \rightarrow \Gamma_{3,1}^c$ ,  $\Gamma_1^c$  transitions, respectively. The closing of the gap is interpreted in terms of pressure-induced enhancement of the interlayer-interaction broadening of intralayer bands, which is a common characteristic of semiconducting layer material. Finally, the possibility of a structural phase transition at about 1.85 GPa is indicated by our data, but they cannot provide a conclusive answer.

#### ACKNOWLEDGMENTS

We are indebted to Professor M. Cardona and Professor K. Syassen of the Max-Planck-Institut for their hospitality at their laboratories, where the absorption measurements were performed. We would also like to thank W. Dieterich for technical assistance.

- <sup>1</sup>I. A. Karpovich, A. A. Chervova, and L. I. Demidova, Bull. Acad. Sci. USSR, Inorg. Matter **10**, 1899 (1974).
- <sup>2</sup>G. B. Abdullaeva, K. R. Allakhverdiev, R. Kh. Nani, E. Yu. Salaev, and R. M. Sardarly, Phys. Status Solidi **34**, K115 (1976).
- <sup>3</sup>A. D. Bakhyshev, L. G. Masaeva, A. A. Lebedev, and M. A. Vakobson, Fiz. Tekh. Poluprovodn. **9**, 1548 (1975) [Sov. Phys.—Semicond. **9**, 1021 (1976)].
- <sup>4</sup>K. J. Range, G. Mahlberg, and S. Obenland, Z. Naturforsch. **32b**, 1354 (1977).
- <sup>5</sup>A. E. Bakhyshev, S. Boules, F. E. Fartadzhov, M. Sh. Mamedov, and V. I. Tagirov, Phys. Status Solidi B **95**, K121 (1979).
- <sup>6</sup>E. A. Vinogradov, G. N. Zhizhin, N. N. Melnik, S. I. Subbotin, V. V. Panfilov, K. R. Allakhverdiev, E. Yu. Salaev, and R. Kh. Nani, Phys. Status Solidi B **95**, 383 (1979).
- <sup>7</sup>S. G. Abdullaeva, G. L. Belenkii, and N. T. Mamendov, Phys.

- Status Solidi B **102**, K19 (1980).
- <sup>8</sup>S. G. Abdullaeva, G. L. Belenkii, M. O. Godzhaev, and N. T. Mamedov, Phys. Status Solidi B **103**, K61 (1981).
- <sup>9</sup>S. G. Abdullaeva, G. L. Belenkii, and N. T. Mamendov, Fiz. Tekh. Poluprovodn. **15**, 943 (1981) [Sov. Phys.—Semicond. **15**, 540 (1981)].
- <sup>10</sup>W. Henkel, H. D. Hochheimer, C. Carlone, A. Werner, S. Ves, and H. G. v. Schnering, Phys. Rev. B **26**, 3211 (1982).
- <sup>11</sup>S. G. Abdullaeva, N. T. Mamedov, and G. S. Orudzhev, Phys. Status Solidi B **119**, 11 (1983).
- <sup>12</sup>K. R. Allakhverdiev, S. S. Babaev, N. A. Bakhyshev, T. G. Mamedov, E. Yu. Salaev, and I. K. Efendieva, Phys. Status Solidi B **126**, K139 (1984).
- <sup>13</sup>R. A. Aliev, K. R. Allakhverdiev, A. I. Baranov, N. R. Ivanov, and R. M. Sardarly, Fiz. Tverd. Tela (Leningrad) **26**, 1271 (1984) [Sov. Phys.—Solid State **26**, 775 (1984)].
- <sup>14</sup>K. R. Allakhverdiev, T. G. Mamedov, G. I. Peresada, E. G.

- Ponyatovskii, and Ya. N. Sharifov, *Fiz. Tverd. Tela (Leningrad)* **27**, 927 (1985) [*Sov. Phys.—Solid State* **27**, 568 (1985); **27**, 3178 (1985) [**27**, 10 (1985)].
- <sup>15</sup>K. R. Allekhverdiev, S. S. Babaev, N. A. Bakhyshov, and T. G. Mamedov, *Fiz. Tverd. Tela (Leningrad)* **27**, 3699 (1985).
- <sup>16</sup>F. M. Gashimzade, B. R. Gadzhiev, K. R. Allakhverdiev, R. M. Sardarly, and V. Ya. Shteinshraiber, *Fiz. Tverd. Tela (Leningrad)* **27**, 2286 (1985) [*Sov. Phys.—Solid State* **27**, 1372 (1985)].
- <sup>17</sup>V. A. Aliev and G. D. Guseinov, *Fiz. Tekh. Poluprovodn.* **19**, 1940 (1985) [*Sov. Phys. Semicond.* **19**, 1195 (1985)].
- <sup>18</sup>K. R. Allakhverdiev, T. G. Mamedov, V. V. Panfilov, M. M. Shukyurov, and S. I. Subbotin, *Phys. Status Solidi B* **131**, K23 (1985).
- <sup>19</sup>G. I. Abutalybov, I. Kh. Akopyan, I. K. Neimanzade, B. V. Novikov, and E. Yu. Salaev, *Fiz. Tverd. Tela (Leningrad)* **27**, 2836 (1985) [*Sov. Phys.—Solid State* **27**, 1710 (1985)].
- <sup>20</sup>K. R. Allakhverdiev, M. A. Aldzanov, T. G. Mamedov, and E. Yu. Salaev, *Solid State Commun.* **58**, 295 (1986).
- <sup>21</sup>S. G. Guseinov, G. D. Guseinov, N. Z. Gasanov, and S. B. Kyazimov, *Phys. Status Solidi B* **133**, K25 (1986).
- <sup>22</sup>S. G. Abdullaeva and N. T. Mamedov, *Phys. Status Solidi B* **133**, 171 (1986).
- <sup>23</sup>Sh. Nurov, V. M. Burlakov, E. A. Vinogradov, N. M. Gasanly, and B. M. Dzhavadov, *Phys. Status Solidi B* **137**, 21 (1986).
- <sup>24</sup>T. D. Ibragimov and N. T. Mamedov, *Phys. Status Solidi B* **145**, K103 (1988).
- <sup>25</sup>A. A. Volkov, Yu. G. Concharov, G. V. Kozlov, S. P. Lebedev, A. M. Prokhorov, R. A. Aliev, and K. R. Allekhverdiev, *Pis'ma Zh. Eksp. Teor. Fiz.* **37**, 517 (1983) [*JETP Lett.* **37**, 615 (1983)].
- <sup>26</sup>B. Welber, M. Cardona, C. K. Kim, and S. Rodriguez, *Phys. Rev. B* **12**, 5729 (1975).
- <sup>27</sup>B. Welber, M. Cardona, Y. F. Tsay, and B. Bendow, *Phys. Rev. B* **15**, 875 (1977).
- <sup>28</sup>S. Ves, K. Strössner, C. K. Kim, and M. Cardona, *Solid State Commun.* **55**, 327 (1985).
- <sup>29</sup>K. Strössner, S. Ves, C. K. Kim, and M. Cardona, *Phys. Rev. B* **33**, 4014 (1986).
- <sup>30</sup>K. Strössner, S. Ves, C. K. Kim, and M. Cardona, *Solid State Commun.* **61**, 275 (1987).
- <sup>31</sup>S. Ves, D. Glötzel, H. Overhof, and M. Cardona, *Phys. Rev. B* **24**, 3073 (1981).
- <sup>32</sup>A. R. Goni, K. Strössner, K. Syassen, and M. Cardona, *Phys. Rev. B* **36**, 1581 (1987).
- <sup>33</sup>A. R. Goni, K. Syassen, K. Strössner, and M. Cardona (unpublished).
- <sup>34</sup>D. Barnett, S. Block, and J. C. Piermarini, *Rev. Sci. Instrum.* **44**, 1 (1973).
- <sup>35</sup>S. Hawke, K. Syassen, and W. J. Holzapfel, *Rev. Sci. Instrum.* **45**, 1548 (1974).
- <sup>36</sup>J. M. Besson, J. Gernogora, and R. Zallen, *Phys. Rev. B* **22**, 3866 (1980).
- <sup>37</sup>A. Morita and T. Sasaki, in *Proceedings of the 18th International Conference on the Physics of Semiconductors*, edited by O. Engstrom (World Scientific, Stockholm, 1987), pp. 1847ff.
- <sup>38</sup>G. R. Valyukonis, A. S. Medeishis, and A. Yu. Shileika, *Fiz. Tekh. Poluprovodn.* **16**, 1137 (1982) [*Sov. Phys. Semicond.* **16**, 73 (1982)].
- <sup>39</sup>J. M. Besson, K. P. Jain, and A. Kuhn, *Phys. Rev. Lett.* **32**, 936 (1974).
- <sup>40</sup>G. D. Guseinov, A. V. Malsagov, A. Kh. Matiev, S. Kh. Umarov, E. G. Abdujlaev, and M. L. Shubnikov, *Fiz. Tekh. Poluprovodn.* **18**, 885 (1985) [*Sov. Phys. Semicond.* **19**, 545 (1985)].
- <sup>41</sup>B. A. Weinstein, R. Zallen, M. L. Slade, and A. deLozanne, *Phys. Rev. B* **24**, 4652 (1981).
- <sup>42</sup>M. Kastner, *Phys. Rev. B* **6**, 2273 (1972); **7**, 5237 (1973); M. Kastner and R. R. Forberg, *Phys. Rev. Lett.* **36**, 740 (1976).
- <sup>43</sup>R. Zallen and D. F. Blossey, in *Physics and Chemistry of Materials with Layered Structure*, Vol. 4 of *Optical and Electrical Properties*, edited by P. A. Lee (Reidel, Dordrecht, 1976), pp. 248ff.
- <sup>44</sup>K. Strössner, S. Ves, and M. Cardona, *Phys. Rev. B* **32**, 6614 (1985).
- <sup>45</sup>F. M. Gashimzade and G. S. Orudzhev, *Phys. Status Solidi B* **106**, K67 (1981).